Electronic Supplementary Information

Target-triggered cascade assembly of catalytic network as artificial enzyme for highly efficient sensing

Lei Zhang,† Fengjiao Ma,† Jianping Lei,* Jintong Liu and Huangxian Ju*

State Key Laboratory of Analytical Chemistry for Life Science, School of Chemistry and Chemical Engineering, Nanjing University, Nanjing 210023, P.R. China

*Address correspondence to jpl@nju.edu.cn, hxju@nju.edu.cn

This PDF file includes:

Materials and Reagents

Chloroauric acid ($HAuCl_4 \bullet 4H_2O$), 2,4,6-pyrimidinetrione and hydrogen peroxide were purchased from Sinopharm Chemical Reagent Co., Ltd. (China). Pamidronic acid disodium salt (PADS) and 1-hydroxyethane-1,1-diphosphonic acid (HEDP) were obtained from Tokyo Chemical Industry Co., Ltd. 3-Aminopropylphosphonic acid (APPA), hemin, xanthine, xanthine oxidase, 4-imidazolecarboxaldehyde, 4-pyridinecarboxaldehyde, tyramine, pyrogallol, N-(3-dimethylaminopropyl)-N'-ethylcarbodiimide hydrochloride (EDC), 2,2'-azobis(2-amidinopropane) dihydrochloride (AAPH), *o*-phenylenediamine, and 3-(4,5-dimethyl-2-thiazolyl)-2,5-diphenyl-2-H-tetrazolium bromide (MTT) were purchased from Sigma-Aldrich (USA). HS-poly(ethylene glycol) (PEG) (M.W. 3400) was obtained from Nanocs (USA). Phosphate buffer saline (PBS, pH 7.4) contained 136.7 mM NaCl, 2.7 mM KCl, 8.72 mM Na_2HPO_4 and 1.41 mM KH_2PO_4. All other reagents were of analytical grade. All aqueous solutions were prepared using ultrapure water (≥ 18 MΩ, Milli-Q, Millipore).

Apparatus

Absorption spectra were recorded on an UV-3600 UV-Vis-NIR spectrophotometer (Shimadzu, Japan). The transmission electron microscopic (TEM) images were obtained on a JEM-2100 transmission electron microscope (JEOL Ltd., Japan). X-ray photoelectron spectroscopic (XPS) experiments were operated on an ESCALAB 250 spectrometer (Thermo-VG Scientific Co., USA) with an ultrahigh vacuum generator. Dynamic light scattering (DLS) was observed on a 90 Plus/BI-MAS equipment (Brook Haven, USA). Zeta potential analysis was performed on a

Zetasizer instrument (Nano-Z, Malvern, UK). Infrared (IR) spectra were recorded on a Nicolet NEXUS870 Fourier transform infrared (FT-IR) spectrometer (Madison, WI). Fluorescence spectra were measured on an F-7000 spectrometer (HITACHI, Japan). Confocal fluorescence imaging of cells was performed on a TCS SP5 confocal laser scanning microscope (Leica, Germany). Electrospray ionization mass spectrum (ESI-MS) was recorded on an Agilent G6540Q-TOF LC/MS equipped with an ESI probe operating in positive ion mode. Matrix-assisted laser desorption/ionization time-of-fight mass spectrometry (MALDI-TOF-MS) experiments were performed on a 4800 Plus MALDI TOF/TOF Analyzer (AB Sciex, U.S.A.) with the Nd:YAG laser at 355 nm, a repetition rate of 200 Hz and an acceleration voltage of 20 kV. Data analysis was performed with a Data Explorer Software from AB Sciex.

Experimental Section

Synthesis of Au-Hem

All glassware was cleaned in aqua regia (3:1 of HCl/HNO_3), rinsed with ultrapure water, and then dried prior to use. 14 mg mL^{-1} PADS solution was quickly added in 20 mL boiling aqueous solution of $HAuCl_4$ (1%) with a mass ratio of 5.0:1 for PADS:$HAuCl_4$, which resulted in a colour change from pale yellow to colorlessness and then deep red. Afterward, the solution was refluxed for an additional 10 min, and cooled to room temperature for obtaining N-AuNPs. Similar procedure was used for the reaction of $HAuCl_4$ with HEDP or APPA.

Au-Hem was synthesized with a standard carbodiimide chemistry to couple hemin on the N-AuNPs. In brief, 300 μL of 1 mM hemin solution (pH 11), 100 μL of Tween solution (1%), 15 mg of EDC and 0.5 mg of SH-PEG were added in 10 mL of N-AuNPs (2.5 nM) solution and

incubated for 3 h under dark. The reaction solution was centrifuged at 10,000 rpm for 10 min, and the obtained precipitate was washed twice to remove unbound hemin in the supernatant. The resulting **Au-Hem** was resuspended in ultrapure water for further experiments.

Structures of PADS, HEDP and APPA

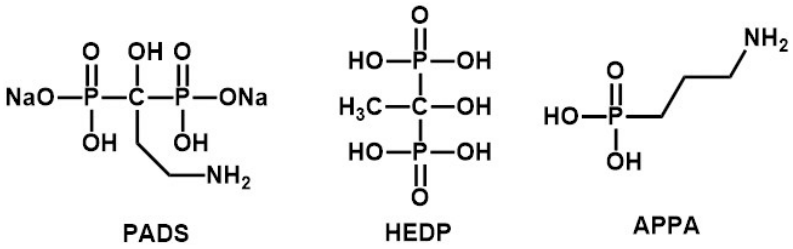

Synthesis of MPT

A mixture of pyrimidinetrione (820 mg, 5.0 mmol), 4-imidazolecarboxaldehyde (480 mg, 5.0 mmol), and piperidine (1 mL) in methanol (10 mL) was refluxed under nitrogen atmosphere for about 5 h (Reaction 1). After the colour turned from faint yellow to orangered, the solid was collected by filtration, washed with methanol and dried under vacuum to give an orangered precipitate of **MPT**. Yield: 356 mg, 34.4%. Its characteristic data are as follows. MALDI-TOF-MS: *m*/*z* calculated for $C_8H_6N_4O_3$ + H^+, 207.2; found, 207.0. ^{1}H NMR (500 MHz, D_2O, ppm): 7.859 (s, 1H), 7.529 (s, 1H), 7.510 (s, 1H), 6.647 (s, 1H), 6.409 (s, 1H), 5.357 (s, 1H). ^{13}C NMR (500 MHz, D_2O, ppm): 168.358, 165.757, 153.400, 153.263, 135.443, 134.615, 133.358, 121.501.

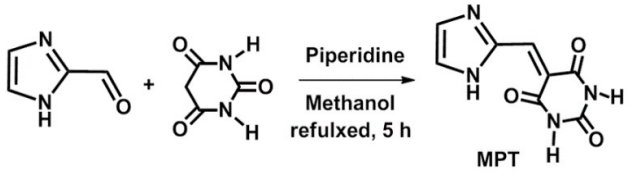

……..(1)

Synthesis of PMPT

A mixture of 2,4,6-pyrimidinetrione (820 mg, 5.0 mmol), 4-pyridinecarboxaldehyde (536 mg, 5.0

mmol), and piperidine (1 mL) in methanol (10 mL) was refluxed under nitrogen atmosphere for about 5 h to obtain the pyridine derivative (**PMPT**, Reaction 2). The color of the reaction solution turned from faint yellow to red and then to reddish brown. The solid was collected by filtration, washed with methanol and dried under vacuum to give a white precipitate. Yield: 436 mg, 40%. The characteristic data of **PMPT** are listed as follows. ESI-MS: *m*/*z* calculated for $C_{10}H_7N_3O_3$ + H^+, 218.2; found, 218.1. ^{1}H NMR (500 MHz, DMSO-d6, ppm): 10.038 (s, 2H), 8.315 (d, 2H, J = 6.0 Hz), 6.993 (d, 2H, J = 6.0 Hz), and 5.965 (s, 1H). ^{13}C NMR (500 MHz, D_2O, ppm): 166.161, 165.594, 153.211, 146.443, 141.390, 125.001, and 121.571.

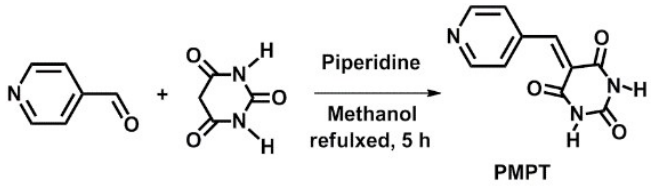

…….(2)

Preparation of Au-Hem-MPT and Au-Hem-Net

Au-Hem-MPT was prepared by mixing **Au-Hem** (0.1 μM equivalent hemin, 9.9 mL) and **MPT** (10 μM, 0.1 mL), and then standing for 1 h at 37 ^{o}C. After addition of Hg^{2+} (0.1 μM) in the obtained **Au-Hem-MPT** (0.1 μM equivalent hemin) for 9 min, the **Au-Hem-Net** was obtained. Similarly, **Au-Hem-PMPT** and **Au-Hem-pNet** (0.2 μM hemin equivalent) were prepared at room temperature.

Evaluation of catalytic activity

The catalytic performance was evaluated through the oxidation of non-fluorescent tyramine by H_2O_2 to form fluorescent dityramine in the presence of corresponding catalyst (Reaction 3). The fluorescence spectra were conducted at an excitation wavelength of 320 nm.

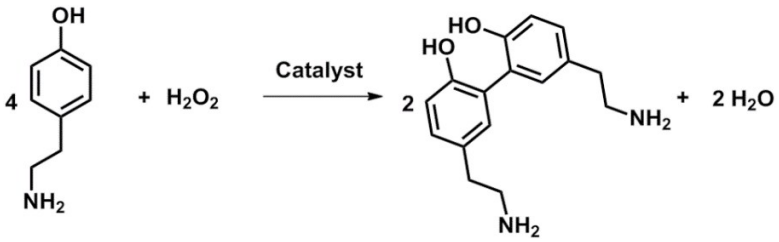

……. (3)

The kinetic studies were carried out using pyrogallol oxidation at room temperature (Reaction 4). The concentration of pyrogallol varied from 0.05 to 0.5 mM with a fixed amount of enzyme mimics (0.2 μM hemin equivalent) and a H_2O_2 concentration of 0.4 mM in pH 7.4 Tris-HCl solution. The reaction was monitored in kinetic mode at 325 nm with a UV-vis spectrometer. The apparent kinetic parameters were calculated with the function $v = V_{max} \times [S]/(K_m+[S])$, where v is the initial velocity, [S] is the substrate concentration, K_m is Michaelis constant, and V_{max} is the maximum reaction velocity. When the concentration of active sites [E] is known and these sites are fully saturated with substrate pyrogallol, the catalytic kinetic constant k_{cat} that is generally defined as the turnover number can be calculated with $V_{max}/[E]$.

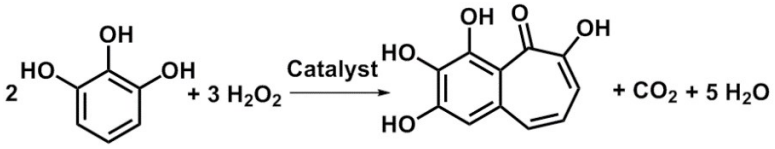

……..(4)

Hemin amount conjugated on nanoparticle

The amount of hemin conjugated on the surface of the nanoparticle was determined by UV-Vis spectroscopy. The absorbance of all the supernatant from the preparation of **Au-Hem** was converted to the concentration of corresponding hemin with a linear calibration curve. The calibration curve was obtained with known concentrations of hemin (Fig. S4B). Finally, the loading amount of hemin on N-AuNPs was obtained by dividing the subtracted concentration by the original N-AuNP concentration.

Preparation of ROS

$^1O_2$ was generated by the reaction of H_2O_2 with NaClO. $O_2^{\cdot-}$ was produced by the enzymatic reaction of xanthine/xanthine oxidase under anaerobic condition at 25 °C for 5 min.[S1] ROO$^{\cdot}$ was generated by AAPH, and $^{\cdot}OH$ was prepared by Fenton reaction ($Fe^{2+} + H_2O_2 \rightarrow Fe^{3+} + {}^{\cdot}OH + OH^-$).[S2] The concentrations of all reactants such as H_2O_2, NaClO, xanthine, xanthine oxidase, AAPH and Fe^{2+} were 0.4 mM.

Cell culture

HeLa cells were cultured in a flask in Dulbecco's modified Eagle's medium (DMEM, Gibco) supplemented with 10% fetal calf serum (FCS, Gibco), penicillin (100 μg mL^{-1}), and streptomycin (100 μg mL^{-1}) at 37 ^{o}C in a humidified atmosphere containing 5% CO_2. Cell number was determined using a Petroff-Hausser cell counter (USA).

MTT assay

The cytotoxicity of **Au-Hem-Net** was examined by MTT assay. Briefly, after HeLa cells (100 μL, 5.0×10^5) were seeded in the wells of 96-well plate for 12 h, the medium was discarded. The cells were then washed twice with PBS, and incubated with 100 μL culture medium containing different amounts of **Au-Hem-Net** (10 nM equivalent hemin) in the presence of 0.14 mM *o*-phenylenediamine for 5 h. Meanwhile, the cells were incubated with 100 μL culture medium without the catalyst and substrate as control. After washing with PBS, MTT (50 μL, 1 mg mL^{-1}) was added to each well, and incubated at 37 ^{o}C for 4 h. The medium was removed, and 150 μL of DMSO was added to each well. After the cell plate was vibrated for 15 min at room temperature to dissolve the crystals formed by the living cells, the absorbance of each well was measured at a wavelength of 560 nm with a microplate reader. The relative cell viability (%) was calculated by

$(A_{test}/A_{control}) \times 100$.

Confocal fluorescence imaging

HeLa cells were seeded into 35-mm confocal dishes (Glass Bottom Dish) at a density of 5.0×10^4 per dish and incubated for 12 h at 37 °C. The medium was then replaced with fresh culture medium containing 0.14 mM *o*-phenylenediamine in the absence/presence of mimic enzyme of **Au-Hem-Net** (10 nM equivalent hemin) and incubated for different times. The fluorescence of cells was visualized with a confocal laser scanning microscope at stationary parameters including the laser intensity, exposure time and objective lens. Prior to imaging, the cells were rinsed three times with PBS and kept in PBS. The cells were excited at 405 nm with a diode laser and the emission was collected from 525 to 575 nm. All images were digitized and analyzed with Leica Application Suite Advanced Fluorescence (LAS-AF) software package.

Supporting Figures

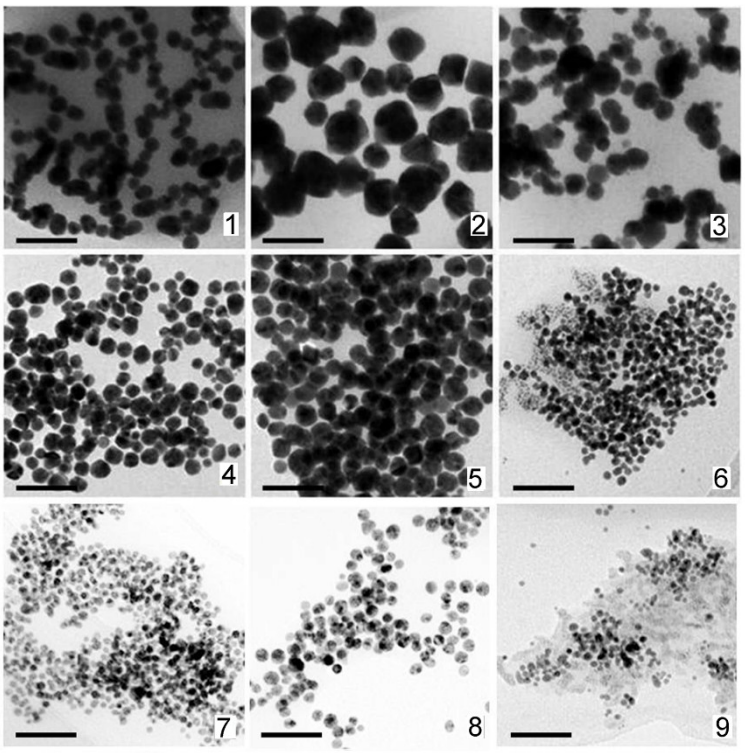

Fig. S1. TEM characterizations of N-AuNPs. TEM images of AuNPs prepared with PADS and $HAuCl_4$ at mass ratios of 2.6, 3.0, 3.2, 5.0, 7.0, 11.0, 26.4, 55.4 and 142.4 (from 1 to 9). Scale bars, 50 nm.

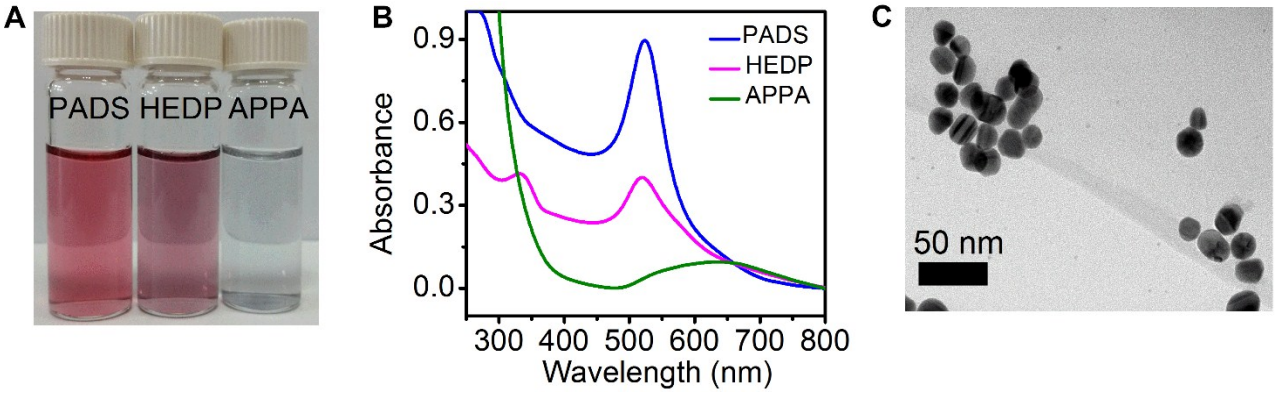

Fig. S2. Comparisons of $HAuCl_4$ reduced by PADS, HEDP and APPA. (**A**) Photographs and (**B**) UV-vis spectra of the reaction solutions of PADS, HEDP and APPA with $HAuCl_4$ at the mass ratio of 5.0:1. (**C**) TEM image of Au nanoparticles prepared by the reaction of HEDP with $HAuCl_4$ at a mass ratio of 5.0:1.

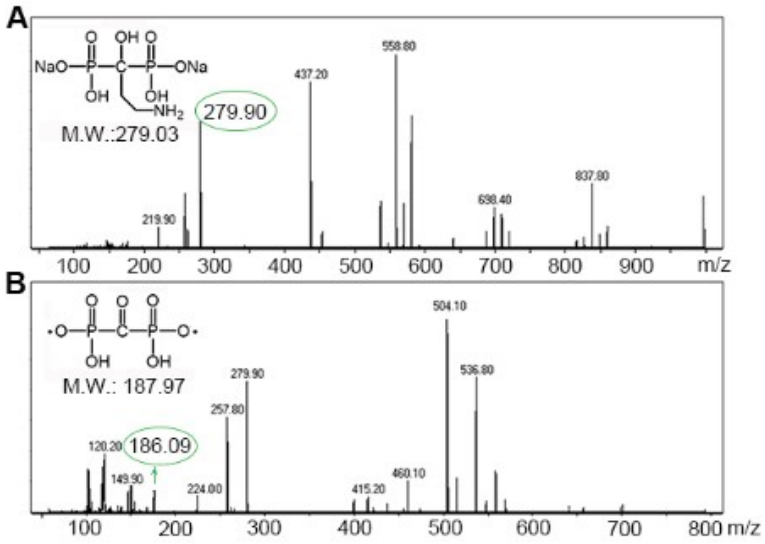

Fig. S3. MS investigation on the reaction of $HAuCl_4$ with PADS. ESI-MS spectra of (**A**) PADS solution and (**B**) reaction solution of $HAuCl_4$ with PADS.

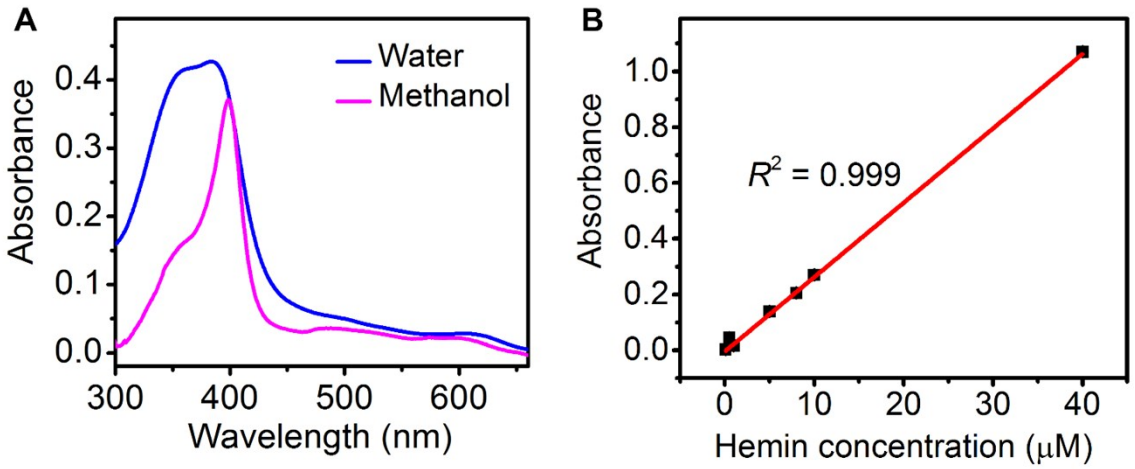

Fig. S4. Spectroscopic properties of hemin. (**A**) UV-vis spectra of hemin in water (blue) and methanol (magenta). (**B**) Plot of absorbance of the Soret band of hemin at 400 nm *vs.* its concentration.

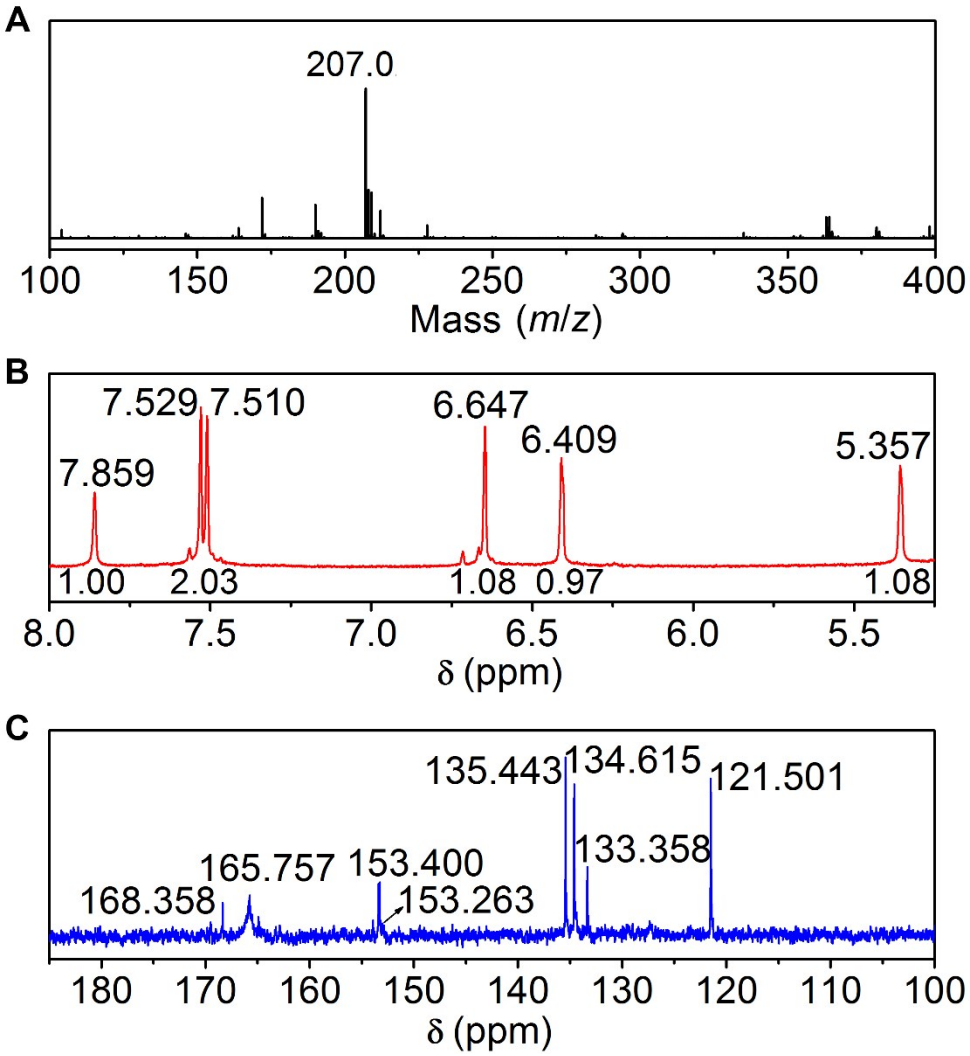

Fig. S5. Characterizations of MPT. MALDI-TOF mass (**A**), ^{1}H NMR (**B**) and ^{13}C NMR (**C**) spectra of **MPT**. The characteristic peak at *m*/*z* 207.0 revealed molecular ion of **MPT** ($[C_8H_7N_4O_3]^+$). The chemical shifts, integrals representing the amount of atomic hydrogen and coupling constants accorded with the **MPT** structure in the ^{1}H NMR spectrum. The chemical shifts in the ^{1}C NMR spectrum were also corresponding to compound.

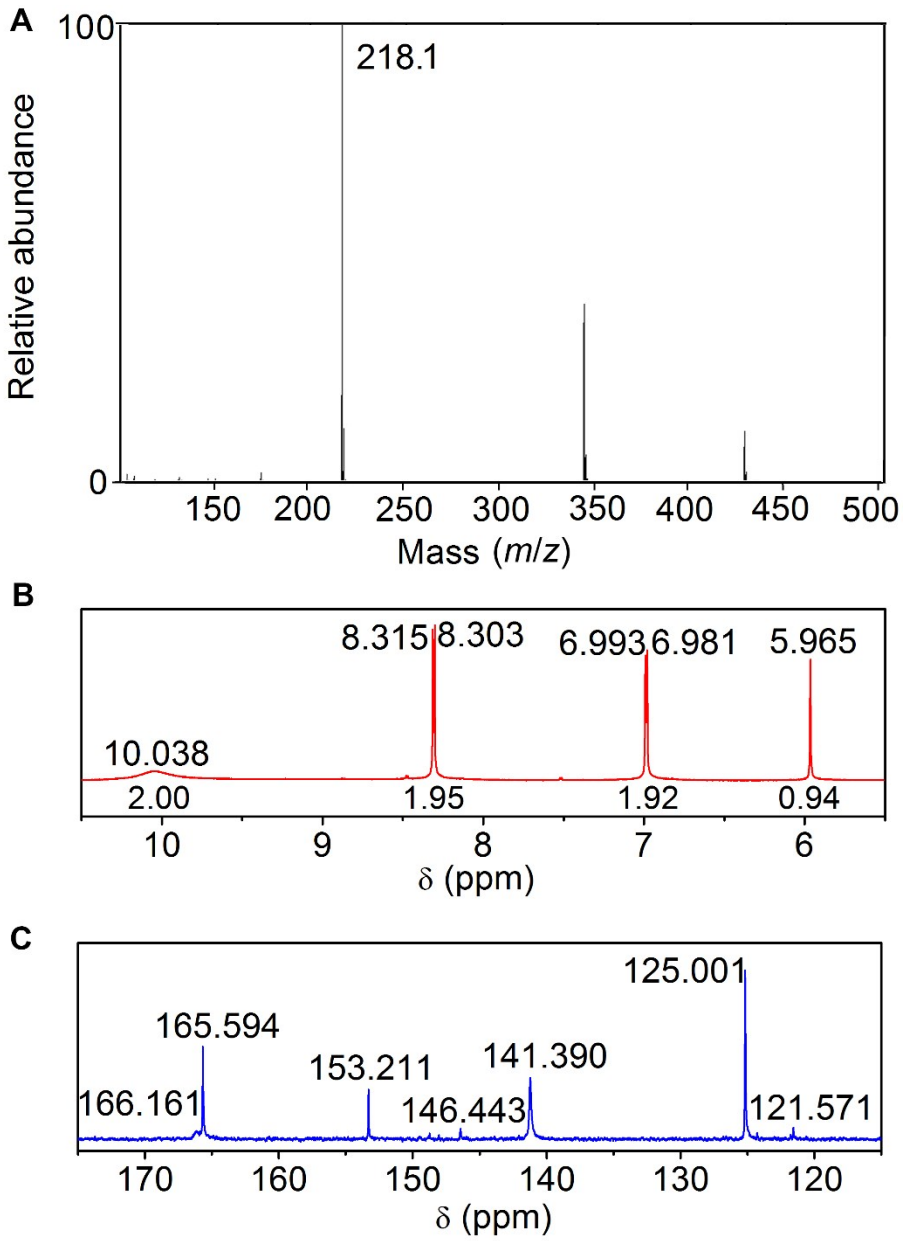

Fig. S6. Characterizations of PMPT. MALDI-TOF mass (**A**), ^{1}H NMR (**B**) and ^{13}C NMR (**C**) spectra of **PMPT**. The characteristic peak at *m/z* 218.1 revealed molecular ion of **PMPT** ($[C_{10}H_8N_3O_3]^+$). The chemical shifts, integrals representing the amount of atomic hydrogen and coupling constants accorded with the **PMPT** structure in the ^{1}H NMR spectrum. The chemical shifts in the ^{1}C NMR spectrum were also corresponding to compound.

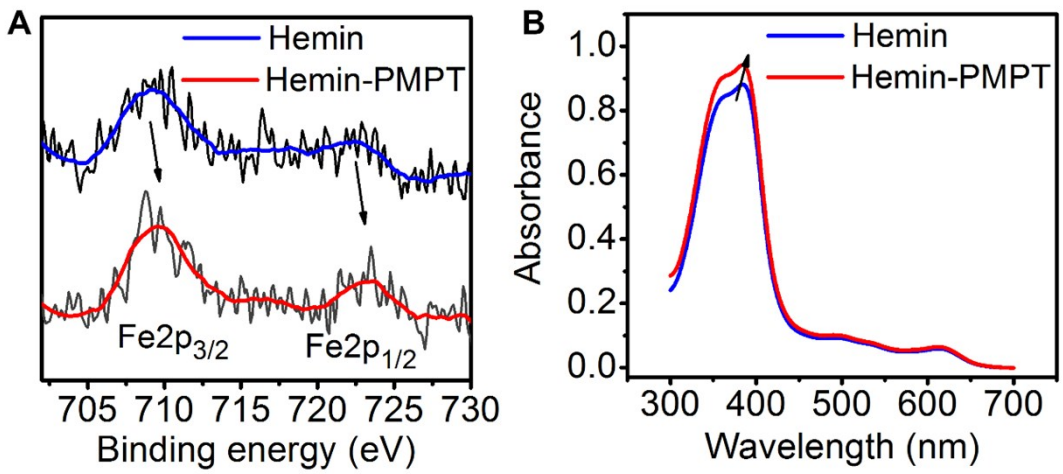

Fig. S7. Axial coordination of PMPT to hemin. (**A**) Fe 2*p* XPS of hemin and hemin-**PMPT** complex. (**B**) UV-vis spectral change upon addition of **PMPT** (100 μM) to hemin (20 μM) in pH 7.4 tris-HCl.

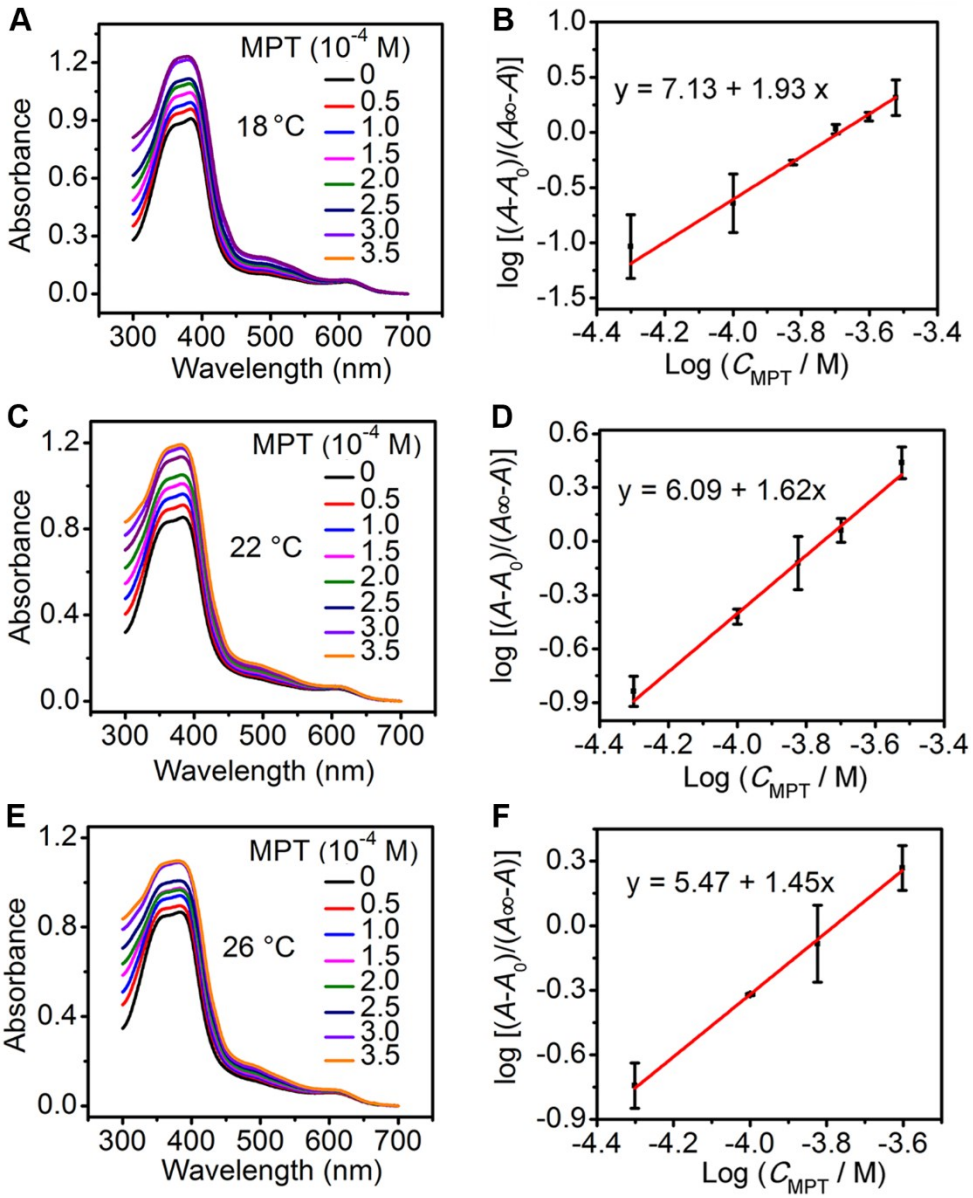

Fig. S8. Calculations of thermodynamic constant. UV-vis spectral change upon titration of **MPT** to hemin (20 μM) in pH 7.4 tris-HCl and corresponding plot of log [(A - A_0)/(A_∞ - A)] *vs.* log $C_{\mathbf{MPT}}$ at 18 (**A**, **B**), 22 (**C**, **D**) and 26 °C (**E**, **F**).

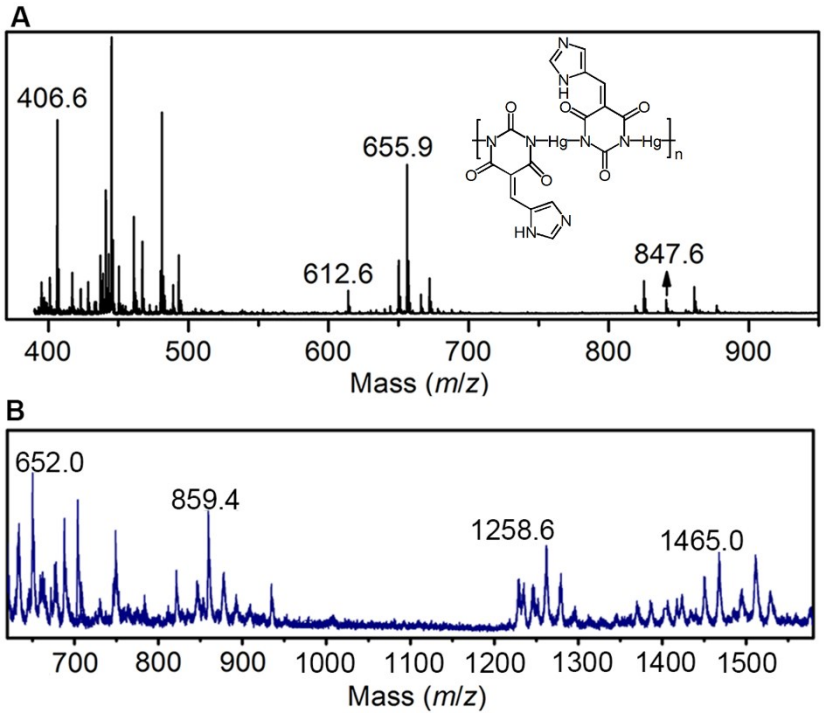

Fig. S9. MALDI-TOF characterization of MPT-Hg^{2+} and Au-Hem-MPT in presence of Hg^{2+}. MALDI-TOF mass spectrum recorded in the positive mode for (**A**) **MPT**-Hg^{2+} adduct and (**B**) **Au-Hem-MPT** (0.1 μM equivalent hemin) in presence of Hg^{2+} (0.1 μM). Inset in (**A**): Proposed structure of **MPT**-Hg^{2+} coordination polymer.

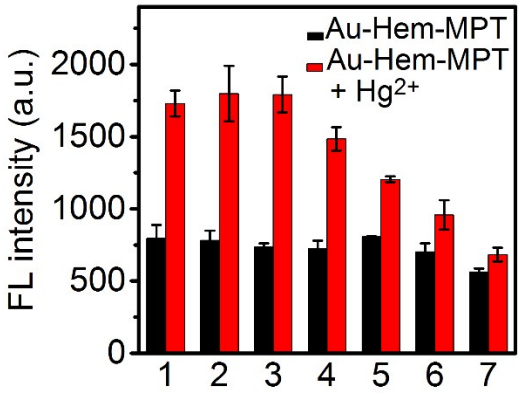

Fig. S10. Catalytic performance of catalyst prepared from different sized N-AuNPs. Fluorescence intensities of oxidation product of tyramine (0.14 mM) catalyzed by **Au-Hem-MPT** (10 nM equivalent hemin) in absence/presence of Hg^{2+} (1.0 nM) based on different sized N-AuNPs (26.1, 19.2, 17, 16.2, 9.4, 8.1 and 6.4 nm, from 1 to 7, respectively) in presence of H_2O_2 (0.4 mM).

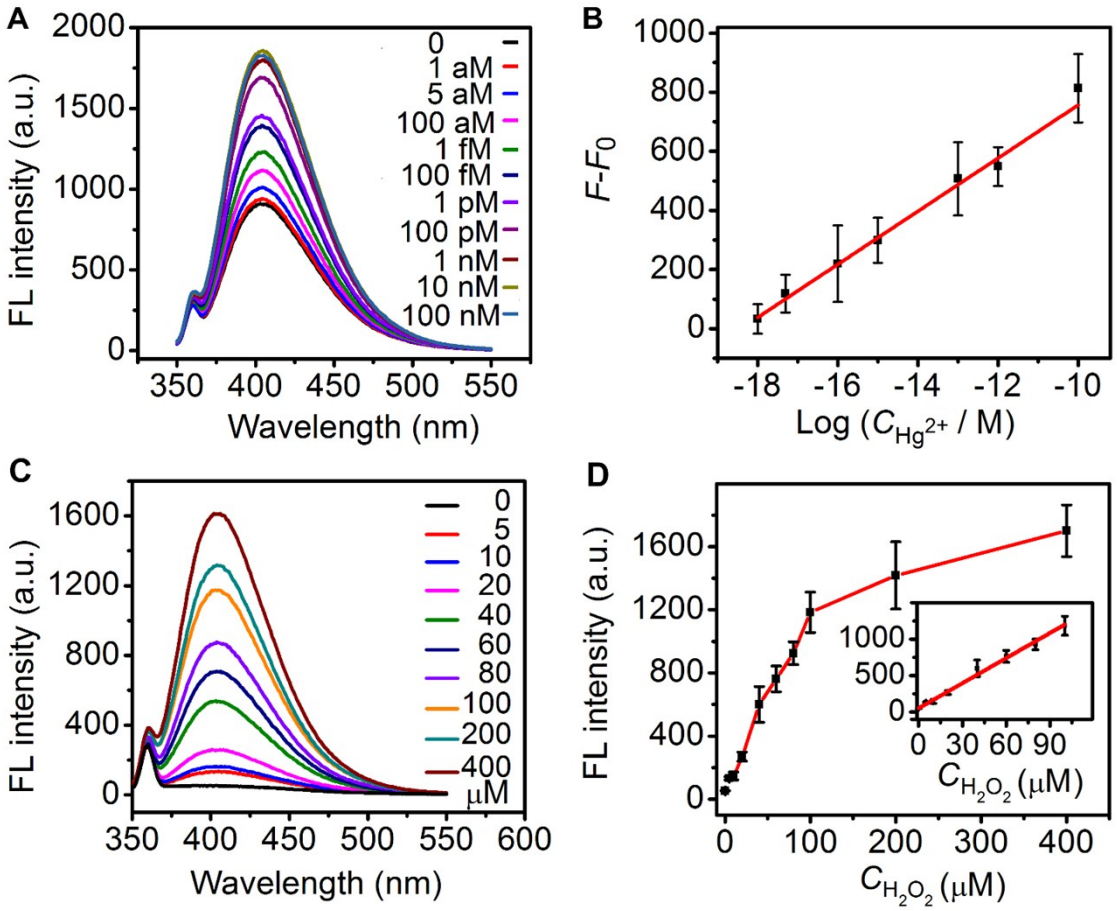

Fig. S11. Analytical performance of Au-Hem-PMPT to Hg^{2+} and Au-Hem-Net in detection of H_2O_2. (**A**) Fluorescence spectra of oxidation product of tyramine (0.14 mM) catalyzed by **Au-Hem-pNet** (10 nM equivalent hemin) prepared at marked Hg^{2+} concentrations in the presence of 0.4 mM H_2O_2 for 15 min. (**B**) Plot of F-F_0 *vs.* logarithm of Hg^{2+} concentration. Here, F_0 and F are the fluorescence intensities obtained in the absence and presence of Hg^{2+}, respectively. (**C**) Fluorescence spectra of oxidation product of tyramine (0.14 mM) catalyzed by **Au-Hem-Net** (10 nM equivalent hemin) in presence of H_2O_2 at marked concentrations at 37 °C for 15 min. (**D**) Plot of fluoresence intensity *vs.* H_2O_2 concentration. Inset, linear plot.

Supplementary Tables

Table S1. TEM and DLS diameters, and Zeta potentials of the N-AuNPs prepared at different mass ratios of PADS to $HAuCl_4$.

Mass ratio	2.6	3.0	3.2	5.0	7.0	11.0	26.4	55.4	142.4
TEM (nm)	16.2	32.4	26.1	16.3	19.2	8.1	8.4	14.2	6.4
DLS (nm)	30.6 ± 7.3	29.1 ± 9.8	30.5 ± 3.0	17.9 ± 3.5	21.1 ± 4.1	15.6 ± 2.4	9.4± 0.9	19.6 ± 2.9	4.8 ± 2.6
Zeta potential (mV)	-14.0± 2.8	-40.4± 7.6	-44.4± 0.7	-48.1± 2.7	-20.0± 6.3	-17.2± 4.7	-21.1± 5.0	-35.2± 1.1	-27.2± 3.6

Table S2. Coordination constants of hemin-MPT and hemin-PMPT complexes.

hemin-**MPT**	Temperature	18 °C	22 °C	26 °C	36 °C
	Coordination number	1.93	1.62	1.45	1.11
	log *K*	7.13	6.09	5.47	3.88
hemin-**PMPT**	Temperature	15 °C	20 °C	28 °C	32 °C
	Coordination number	0.99	1.01	1.13	1.04
	log *K*	5.79	5.51	4.59	3.63

Table S3. Performance of different Hg(II) detection methods.

Detection strategy	Detectable range	Detection limit	ref
Mimetic catalysis of **Au-Hem-Net**	1.0 aM~10 pM	0.3 aM	This work
Hairpin structure induced FRET[a]	40~100 nM	40 nM	S3
Allosteric DNAzyme beacon-based FRET	-[b]	2.4 nM	S4
Gold nanoparticle enhanced fluorescence polarization	1.0 nM~1.0 mM	1.0 nM	S5
Rhodamine-based fluorescent and colorimetric chemodosimeter	5.0~60 nM	5.0 nM	S6
Vinyl ether oxymercuration-based fluorogenic probe	20 nM~1.5 μM	20 nM	S7
Colorimetry using DNA-functionalized gold nanoparticles	0.1~2.0 μM	100 nM	S8
Electrochemical sensor based on hybrid nucleic acid/protein structure	0.1 nM~1.0 μM	100±10 pM	S9
Electrochemical sensor using oligonucleotide probe and gold nanoparticle amplification	0.5~100 nM	0.5 nM	S10
Electrochemiluminescent biosensor	50 pM~10 nM	20 pM	S11
Chemiluminescence of hemin/G-quadruplexes	12.5 nM~1.0 μM	10 nM	S12
Surface-enhanced Raman scattering of nanoporous gold	1.0 nM~10 μM	1.0 pM	S13
Graphene-based field-effect transistor	10 pM~100 nM	10 pM	S14

[a] Fluorescence resonance energy transfer. [b] Not applicable.

Supporting References

S1. I. Ioannidis, M. Bätz, T. Paul, H. G. Korth, R. Sustmann and H. De Groot, *Biochem. J.*, 1996, **318**, 789–795.

S2. H. H. Fenton, *Chem. News.*, 1876, **33**, 190.

S3. A. Ono and H. Togashi, *Angew. Chem. Int. Ed.*, 2004, **43**, 4300–4302.

S4. J. W. Liu and Y. Lu, *Angew. Chem. Int. Ed.*, 2007, **46**, 7587–7590.

S5. B. C. Ye and B. C. Yin, *Angew. Chem. Int. Ed.*, 2008, **47**, 8386–8389.

S6. Y. K. Yang, S. K. Ko, I. Shin and J. Tae, *Nat. Protoc.*, 2007, **2**, 1740–1745.

S7. S. Ando and K. Koide, *J. Am. Chem. Soc.*, 2011, **133**, 2556–2566

S8. J. S. Lee, M. S. Han and C. A. Mirkin, *Angew. Chem. Int. Ed.*, 2007, **46**, 4093–4096.

S9. G. Mor-Piperberg, R. Tel-Vered, J. Elbaz and I. Willner, *J. Am. Chem. Soc.*, 2010, **132**, 6878–6879.

S10. Z. Q. Zhu, Y. Su, J. Li, D. Li, J. Zhang, S. Song, Y. Zhao, G. Li and C. H. Fan, *Anal. Chem.*, 2009, **81**, 7660–7666.

S11. C. X. Tang, Y. Zhao, X. W. He and X. B. Yin, *Chem. Commun.*, 2010, **46**, 9022–9024.

S12. R. Freeman, X. Q. Liu and I. Willner, *J. Am. Chem. Soc.*, 2011, **133**, 11597–11604.

S13. L. Zhang, H. X. Chang, A. Hirata, H. K. Wu, Q. K. Xue and M. W. Chen, *ACS Nano*, 2013, **7**, 4595–4600.

S14. J. H. An, S. J. Park, O. S. Kwon, J. Bae and J. Jang, *ACS Nano*, 2013, **7**, 10563–10571.